*Chemistry for Sustainable Development* **17** (2009) 133–141

UDC 541.136+546.34+544.463

# Application of Mechanical Activation for the Synthesis of Cathode Materials Based on Solid Solutions

N. V. KOSOVA[1], E. T. DEVYATKINA[1] and A. B. SLOBODKIN[2]

[1]*Institute of Solid State Chemistry and Mechanochemistry, Siberian Branch of the Russian Academy of Sciences, Ul. Kutateladze 18, Novosibirsk 6300128 (Russia)*

[2]*Institute of Chemistry, Far East Branch of the Russian Academy of Sciences, Pr. 100-letiya Vladivostoka 159, Vladivostok 690022 (Russia)*

*E-mail: kosova@solid.nsc.ru*

(Received June 30, 2008; revised July 17. 2008)

## Abstract

Dry, waste-free and energy-saving synthesis of cathode materials for lithium-ion rechargeable batteries based on solid solutions having the composition $LiNi_{1-y}Co_yO_2$ ($y$ = 0.2, 0.4, 0.6, 0.8) was realized. Double hydroxides of nickel and cobalt, as well as anhydrous nickel and cobalt oxides in mixture with lithium hydroxide were used as the initial reagents. It was shown that independently of initial materials the samples are characterized by high dispersity, phase uniformity, and are indexed in the $R\bar{3}m$ space group. With an increase in nickel content, the lattice parameters $a$ and $c$ increase; we observe a good correspondence with Vegard rule for solid solutions in the system $LiNiO_2$–$LiCoO_2$. The bands in the IR spectrum get shifted to lower frequencies as a result of a decrease in covalence in the $(Ni_{1-y}Co_yO_2)_2$ layer. The $^{6,7}$Li NMR spectra contain two components that are shifted both to the positive and to the negative region, and provide evidence of the interaction of lithium ions with $Ni^{3+}$ ions situated in the second and the third coordination spheres. Analysis of the fine structure of the second component of MAS spectra located near 0 ppm showed that nickel ions in $Ni_{1-y}Co_yO_2$ layers are distributed non-uniformly at $0.6 \le (1 - y) \le 0.8$. Such a deviation from the random distribution of Ni/Co has a narrow local character and is not detected by means of XPA but affects the electrochemical characteristics of cathode materials.

**Key words:** mechanical activation, lithium-ion rechargeable batteries, cathode materials $LiNi_{1-y}Co_yO_2$, Li MAS NMR, cycling

## INTRODUCTION

Basic requirements to modern lithium-ion rechargeable batteries include an increase in their capacity and power characteristics, efficiency for high speeds of charge and discharge, decrease in the rate of degradation of characteristics during cycling and storage. These requirements stimulate search for new cathode materials and new methods of their synthesis. Improvement of the power characteristics is promoted by increased electron-ion conductivity and dispersity of materials. With a decrease in particle size, the surface of contacts between the electrode and electrolyte increases and the distance for lithium ion diffusion in the solid phase decreases. This causes acceleration of ion transfer and therefore the processes of charge–discharge in rechargeable batteries. The particles of smaller size possess better adaptability to volume changes during intercalation/extraction of lithium ions, which promotes and increase in the structural stability of cathode materials.

In practice, the most widely used cathode material for lithium ion rechargeable batteries is lithium cobaltite $LiCoO_2$. However, its practical specific discharge capacity accounts for only a half of the theoretical value (120–140 instead of 274 mA · h/g), which is due to the structural and chemical instability of $LiCoO_2$ to high voltage, which restricts the upper volta-

ge limit to 4.2 V. Practical capacity of lithium nickelite $LiCoO_2$ reaches 200 mA · h/g instead of the theoretical value which is 275 mA · h/g. In comparison with $LiCoO_2$, the working voltage for $LiNiO_2$ is somewhat lower, and the discharge curve has a more inclined appearance. Oxygen evolution during $LiNiO_2$ charge to high voltage is substantially lower than that in the case of $LiCoO_2$, due to which the safety of the rechargeable battery increases. At the same time, it is much more difficult to perform the synthesis of stoichiometric $LiNiO_2$ with the absence of cation exchange between the Li and Ni layers than the synthesis of $LiCoO_2$.

The synthesis conditions, electrochemical parameters and cost of the solid solutions $LiNi_{1-y}Co_yO_2$ make them occupy an intermediate position between $LiNiO_2$ and $LiCoO_2$ [1–3]. High electron conductivity of $LiNi_{1-y}Co_yO_2$ provides cycling of these compounds at high rates (high current densities) [4]. The discharge curves characteristics of the solid solutions $LiNi_{1-y}Co_yO_2$ are smoother than those for $LiNiO_2$ [5]. It was established that $Ni^{3+}$ ions are the first to get oxidized (in the region $0.85 < x < 1$), only at higher voltage $Co^{3+}$ ions get oxidized. Quite contrary, according to the XANES data [6], oxidation of Ni and Co ions occurs simultaneously. It was reported that the largest capacity and stability during cycling are exhibited by the solid solutions having the composition with $y = 0.2–0.3$ because a minimal change of volume during charge-discharge is observed for them. The presence of cobalt in $LiNiO_2$ not only improves its discharge characteristics but also increases its thermal stability in the charged state. This is due to the higher Co–O bonding energy in comparison with Ni–O (1067 and 1029 kJ/mol, respectively) [7].

Cathode materials based on $LiNi_{1-y}Co_yO_2$ with good electrochemical characteristics, as a rule, are obtained using solution-based methods (co-precipitation, sol-gel *etc.*). The size of particles and crystallinity are varied by variations of temperature and duration of subsequent annealing. Recently, the dry, waste-free and energy-saving method of mechanical activation (MA) has become widely used for obtaining various functional nanometre-sized materials [8]. Preliminary MA of initial mixtures allows one to reduce temperature and duration of annealing, the number of intermediate stages of the synthesis process and improvement of the uniformity of the final product.

In the present work we studied the crystal, local structure and electrochemical properties of solid solutions having the composition $LiNi_{1-y}Co_yO_2$ ($y$ = 2.0, 4.0, 6.0, 0.8), synthesized from double hydroxides of nickel and cobalt, as well as from anhydrous nickel and cobalt oxides with lithium hydroxide using the MA method.

## EXPERIMENTAL

Mixed hydroxides of nickel and cobalt $LiNi_{1-y}Co_yO_2$ were obtained using the procedure described in [9, 10]. Lithium hydroxide LiOH was obtained from lithium hydroxide monohydrate be annealing at a temperature of 350 °C. Commercially available nickel oxide NiO and cobalt oxide $Co_2O_3$ of ch.d.a. reagent grade were used. Preliminary MA of the mixture of initial reagents was carried out in a planetary activator AGO-2 with water cooling using steel cylinders and balls. Activated mixtures were annealed in a furnace at a temperature of 750 °C.

Thus obtained samples were analyzed by means of X-ray phase analysis, IR and $^{6,7}$Li NMR spectroscopy, scanning electron microscopy and cyclic chronopotentiometry. Structural examination was carried out with DRON-3M diffractometer (Cu$K_\alpha$ radiation). IT spectra were recorded with a FTIR spectrometer of Bomem Co. (Canada) within the range 200–4000 $cm^{-1}$, $^{6,7}$Li NMR spectra were recorded with a solid-state spectrometer Bruker Avance AV-300 ($H_0$ = 7.05 T, $\nu_{mas}$ = 7 kHz), diluted aqueous solution of LiCl was used as the reference. To record NMR spectra, we used Hahn echo procedure ($\tau = 1/\nu_{mas}$ = 143 μs). Electron microscopic images were taken with a scanning electron microscope LEO 1430 VP. Electrochemical tests were performed in semi-elements "cathode + C (Super P, Timcal Co)/$LiPF_6$ + ethylene carbonate + dimethyl carbonate/Li" with polypropylene separators at a rate of $C/10 - C$ (current density 0.3–3.0 mA/$cm^2$) and temperature of 20 °C.

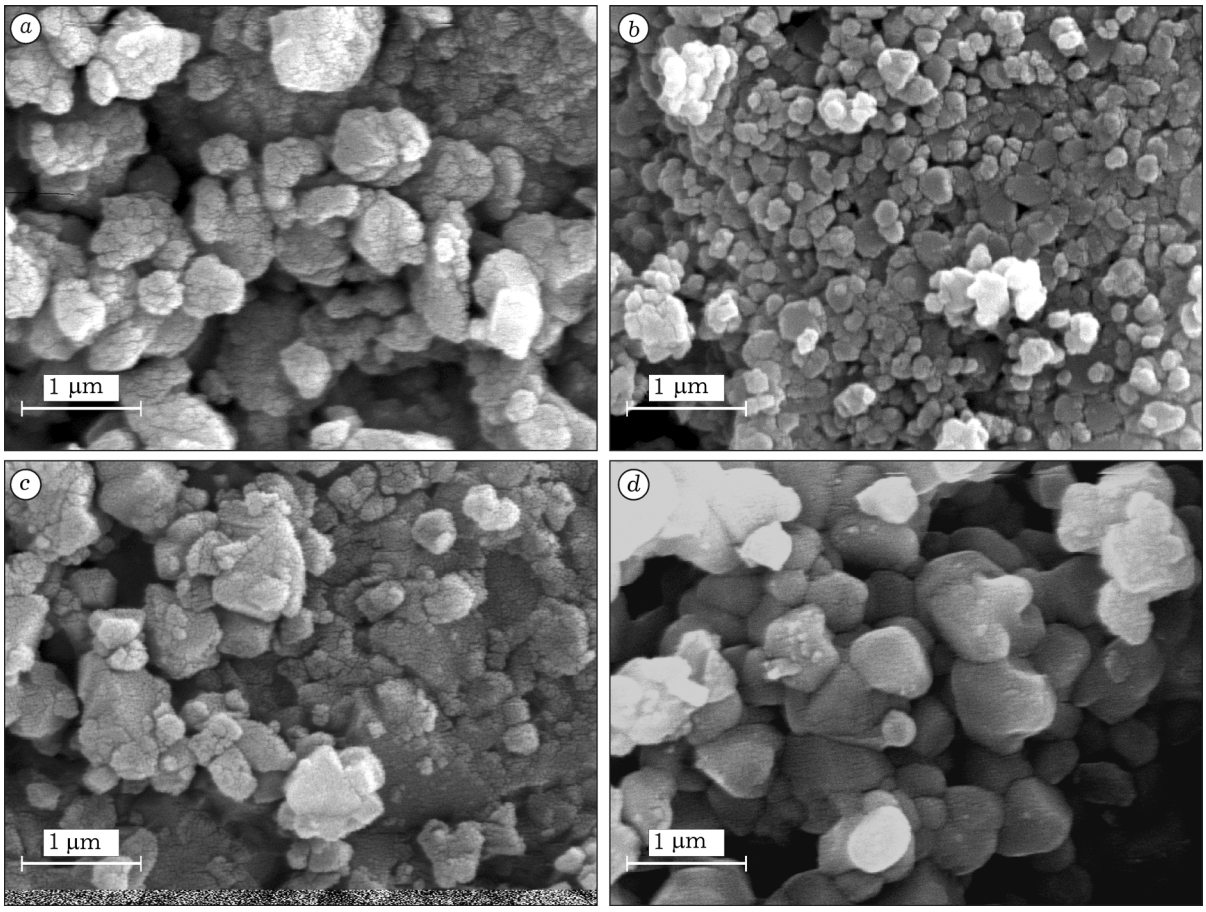


Fig. 1. Micrographs of the particles of $LiNi_{0.8}Co_{0.2}O_2$ (*a*, *c*) and $LiNi_{0.2}Co_{0.8}O_2$ (*b*, *d*) samples obtained from hydroxides (*a*, *b*) and oxides (*c*, *d*) of nickel and cobalt.

**RESULTS AND DISCUSSION**

Micrographs of the particles of $LiNi_{1-y}Co_yO_2$ samples obtained from the hydroxides and oxides of nickel and cobalt are shown in Fig. 1. One can see that the samples are characterized by high dispersity independently of initial reagents. The average size of primary particles is less than 100 nm; primary particles are united into secondary agglomerates less than 500 nm in size. The $LiNi_{1-y}Co_yO_2$ particles obtained from hydroxides have a more rounded shape, and the particle size distribution is narrow in character.

Diffraction patterns of the samples of $LiNi_{1-y}Co_yO_2$ obtained from hydroxides and from oxides are shown in Fig. 2. One can see that all the samples do not contain foreign impurities, that is, they are single-phase. With an increase in nickel content, the crystallinity of samples increases. The samples have layered structure and belong to the space group $R\bar{3}m$ with oxygen packing ABCABC. With an increase in cobalt content, splitting of reflections 006/102 and 018/110 in samples increases, which is the evidence of a decrease in cation disordering between the layers of *d*-metals and lithium because $Co^{3+}$ ions in nickel layers suppress the transition of nickel ions into lithium layers. With an increase in nickel content, lattice parameters *a* and *c* increase (Fig. 3) because $Ni^{3+}$ ions have larger radius than $Co^{3+}$ ions (0.069 and 0.064 nm, respectively). A good correspondence of lattice parameters to Vegard rule for solid solutions in the system $LiNiO_2$–$LiCoO_2$ is observed. The ratio of parameters $c/a$ changes from 4.94 (for $LiNiO_2$) to 4.99 (for $LiCoO_2$).

The IR spectra of $LiNi_{1-y}Co_yO_2$ samples prepared from hydroxides and oxides of nickel and cobalt are presented in Fig. 4. One can see that there are four vibration bands in all the

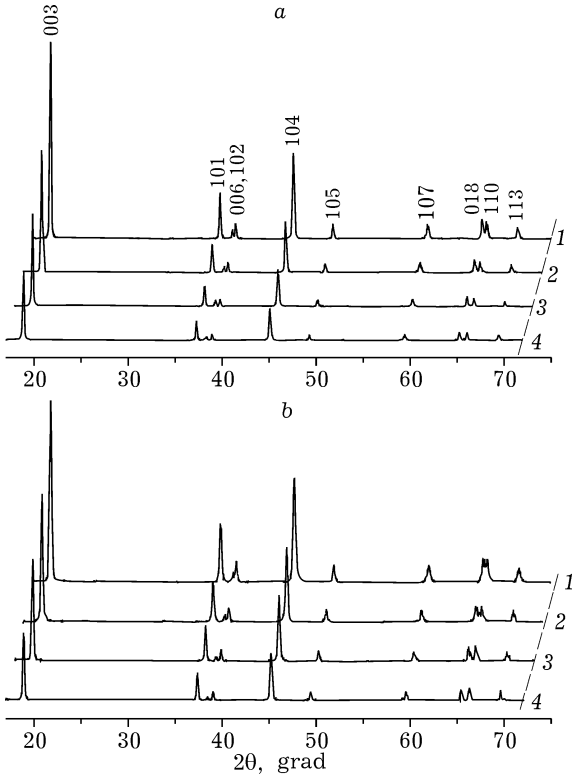


Fig. 2. X-ray diffraction patterns of $LiNi_{1-y}Co_yO_2$ samples obtained from hydroxides (*a*) and oxides (*b*) of nickel and cobalt. The value of $y$: 0.2 (*1*), 0.4 (*2*), 0.6 (*3*), 0.8 (*4*).

spectra. It is known that separate manifestation of $LiO_6$ and $MO_6$ vibration bands is characteristic of $LiNi_{1-y}Co_yO_2$ samples: the bands of $MO_6$ oscillations lie within the region 400–700 $cm^{-1}$, while those of $LiO_6$ are in the region 200–400 $cm^{-1}$ [11]. A comparison of the spectra of samples differing from each other in composition shows that the maxima of bands shift to higher frequencies with an increase in cobalt content. This correlates with changes of cell parameters and the $c/a$ ratio. An increase in the covalence in the $Ni_{1-y}Co_yO_2)_2$ layer with an increase in cobalt content causes a decrease in the metal-metal distance between the layers, which affects band shifts. Broadening of bands in the spectra of samples with high nickel content is due to the presence of cation mixing of two kinds: 1) between the layers of $d$-metals and lithium; 2) in $Ni_{1-y}Co_yO_2)_2$ layers. In spite of the identical X-ray diffraction patterns of the products obtained from hydroxides and oxides, their IR spectra exhibit some differences. In particular, fro all the compositions obtained from oxides, the intensity of bands is much lower.

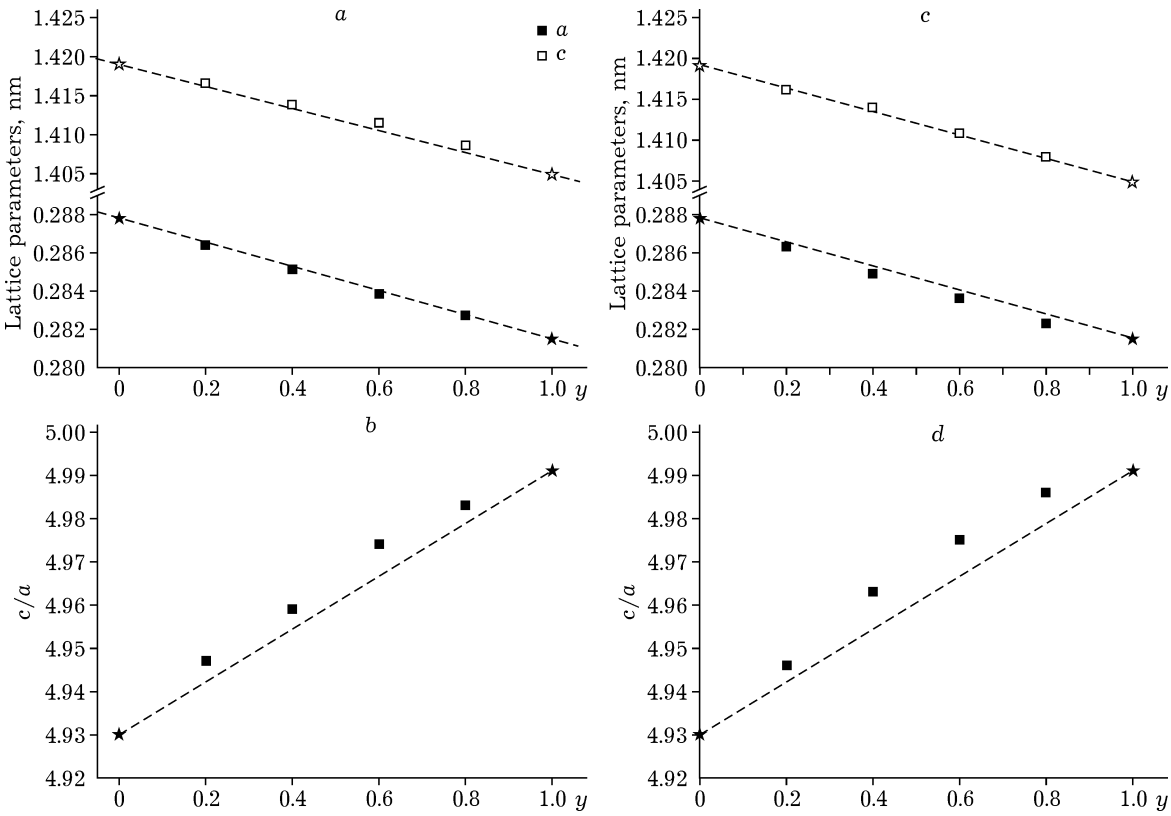


Fig. 3. Parameters of the hexagonal cell $a$ and $c$ and their ratio for $LiNi_{1-y}Co_yO_2$ samples obtained from hydroxides (*a*, *b*) and oxides (*c*, *d*) of nickel and cobalt. Asterisks mark literature data for $LiCoO_2$ and $LiNiO_2$.

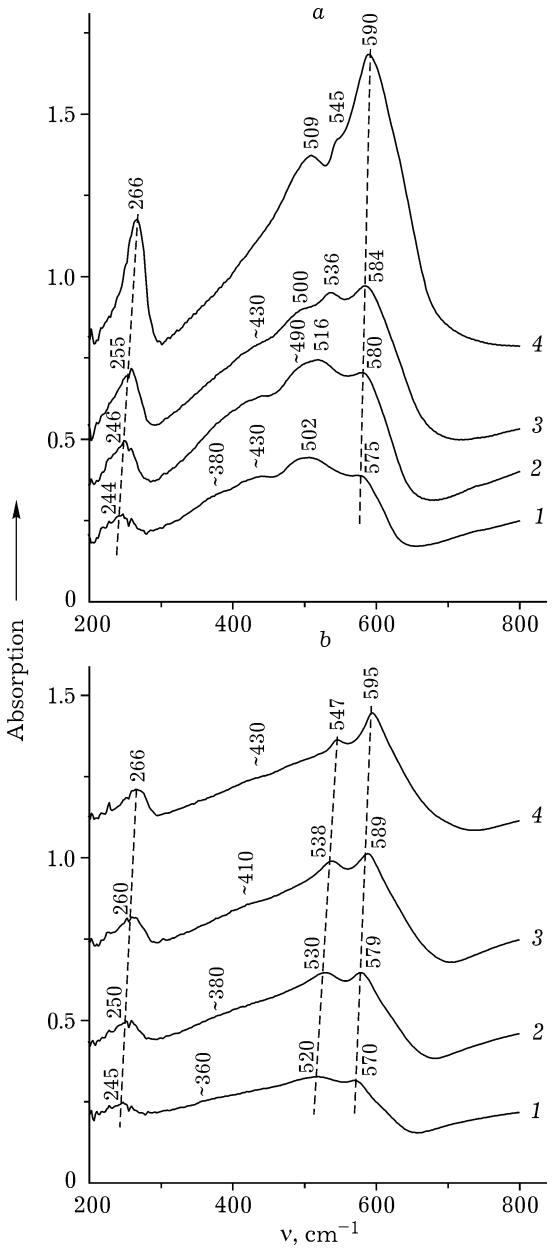


Fig. 4. IR spectra of $LiNi_{1-y}Co_yO_2$ samples obtained from hydroxides (*a*) and oxides (*b*) of nickel and cobalt. The value of $y$: 0.2 (*1*), 0.4 (*2*), 0.6 (*3*), 0.8 (*4*).

To obtain information about the character of the distribution of cobalt ions $Co^{3+}$ ($Co^{3+}$ ($LS\ t_2^6$) and nickel ($Ni^{3+}$ ($LS\ t_2^6e_g^1$) in $Ni_{1-y}Co_yO_2$ layers, we used NMR spectroscopy. The $^{6,7}$NMR studies were carried out with the samples $LiNi_{1-y}Co_yO_2$ ($y$ = 0, 0.2, 0.4, 0.6, 0.8, 1) prepared from nickel and cobalt hydroxides with lithium hydroxide by means of their preliminary MA in ceramic cylinders followed by annealing. The introduction of $Ni^{3+}$ ions into $LiCoO_2$ leads to broadening of static spectra and shift to the positive region; the shift increases with an increase in nickel content of the solid solution (Fig. 5). The spectra contain two components that re shifted both to the positive (component *1*) and to the negative (component *2*) region and provide evidence of the interaction of lithium ions with $Ni^{3+}$ ions that are present in the nearest and the next nearest surroundings of lithium ions (the first and the second coordination spheres) [12–14]. The first signal may be attributed to lithium ions interacting with at least one nickel ion in the nearest surroundings. A narrower signal obtained near 0 ppm and similar to the $LiCoO_2$ signal relates to lithium ions having only $Co^{3+}$ ions in the first coordination sphere. In view of the impossibility to separate these components, in order to analyze the ratio of populations of the indicated positions, the authors of [12] used the position of the centre of gravity or the isotropic shift of the spectrum (σ). The experimental curve is well described by equation $\sigma(y) = C(1 - y)$ where $C$ is the slope coefficient, $(1 - y)$ is nickel content in the solid solution. The isotropic shift is a sum of the contact shift (Fermi) and pseudo-contact shift. In the case of solid solutions $LiNi_{1-y}Co_yO_2$ it is due mainly to the hyperfine shift $p_1\sigma_{hf}$ from $p_1$ of the nearest neighbours of $Ni^{3+}$ ($p_1$ = 0–6) and for the random distribution of Ni/Co can be described with the following equation:

$$\sigma(y) = 6\sigma_{hf}(1 - y)$$

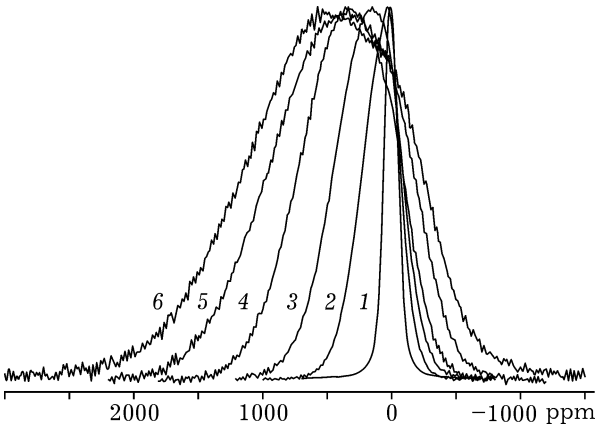


Fig. 5. Static $^7$Li NMR spectra of $LiNi_{1-y}Co_yO_2$ samples obtained from nickel and cobalt hydroxides. The value of $y$: 1 (*1*), 0.8 (*2*), 0.6 (*3*), 0.4 (*4*), 0.2 (*5*), 0 (*6*).

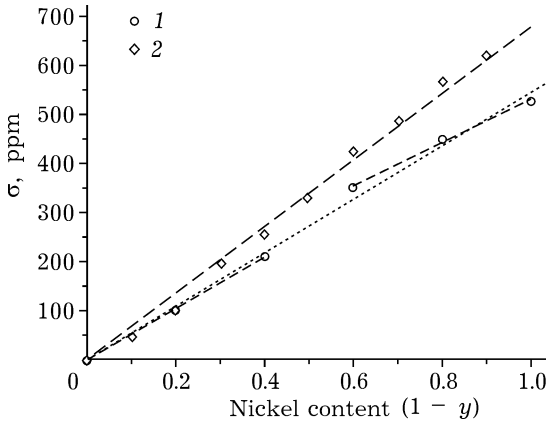


Fig. 6. Dependence of the centre of gravity of $^7$Li NMR spectra (σ) of $LiNi_{1-y}Co_yO_2$ samples on nickel content: *1* – our data, *2* – data reported in [12], linear approximations (shown with dashed lines) for data *1*: $545(1 - y)$ – the whole range, $525(1 - y)$ – the initial region, $443(1 - y) + 88$ – the final region; for data *2* – $679(1 - y)$.

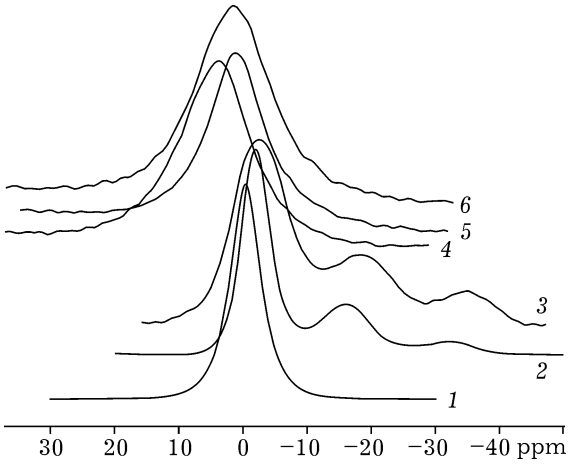


Fig. 7. MAS $^7$Li NMR spectra of $LiNi_{1-y}Co_yO_2$ samples with $y$ equal to 1 (*1*), 0.8 (*2*), 0.6 (*3*), 0.4 (*4*), 0.2 (*5*), 0 (*6*) (highly resolved region).

where $\sigma_{hf}$ is the shift due to the hyperfine interaction of lithium ion with one paramagnetic centre. Taking into account coefficient $C = 679$ ppm determined experimentally in [12], the shift is $\sigma_{hf} = 113$ ppm.

The dependence determined by us $\sigma(y) = C(1 - y)$ is also close to the linear one (Fig. 6), but coefficient $C$ determined by means of the least squares was found to be 545 ppm. In addition, instead of slightly sigmoid form of the $\sigma(y)$ dependence reported in [12], in this case we may assume the presence of discontinuity in the region $0.4 \le (1 - y) \le 0.6$. The initial region is characterized by $C = 525$ ppm and the constant component close to 0, while for the region with $(1 - y) \ge 0.6$ the dependence is described by equation $\sigma(y) = 88 + 443(1 - y)$.

The authors of [12] determined contact shifts (+110 and −15 ppm) from MAS spectra. So, for the ideal $LiNiO_2$ sample in which the number of the nearest neighbours of lithium and the number of neighbours following the nearest ones is 6, the centre of gravity will be $(110 \cdot 6) + (-15 \cdot 6) = 570$ ppm.

The $^{6,7}$Li spectra recorded using the procedure of rotation at the magic angle allow one

TABLE 1

Relative areas ($S$) and chemical shifts (CS) of the components of highly resolved part of the spectra of $LiCoO_2$, $LiNi_{0.2}Co_{0.8}O_2$ and $LiNi_{0.4}Co_{0.6}O_2$ samples

| Samples | $^{6,7}$Li | Peak 1 | | Peak 2 | | Peak 3 | | Calculation* | |
|---|---|---|---|---|---|---|---|---|---|
| | | $S$, % | CS, ppm | $S$, % | CS, ppm | $S$, % | CS, ppm | $q$, % | r.m.s.e., (%)$^2$ |
| $LiCoO_2$ | $^7$Li | 100 | −0.5 | | | | | | |
| $LiNi_{0.2}Co_{0.8}O_2$ | $^7$Li | 64.45 | −1.15 | 30.20 | −14.85 | 5.35 | −31.6 | 7.0 | 0.9 |
| | | (57) | (0) | (32) | (−15) | (11) | (−30) | (9) | (11) |
| | $^6$Li | 55.50 | | 36.00 | | 8.50 | | 9.5 | 4.2 |
| | | (55) | | (36) | | (10) | | (10) | (4) |
| $LiNi_{0.4}Co_{0.6}O_2$ | $^7$Li | 64.25 | −1.70 | 26.85 | −17.00 | 8.85 | −34.0 | 7.0 | 17.0 |
| | | (76) | | (17) | | (6) | | (4) | (27) |
| | $^6$Li | 60.00 | | 24.00 | | 16.00 | | 8.00 | 142.0 |
| | | (58) | | (34) | | (8) | | (9) | (2) |

*Note.* Results of calculations according to the data of [12] are given for comparison in parentheses.

*$q$ is the probability of cobalt substitution by nickel; r.m.s.e. – root-mean-square error.

to observe the fine structure of the component *2* which is situated near 0 (Fig. 7). The $^6$Li spectra give higher solution, while for $^7$Li spectra the signal-to-noise ratio is higher. The data on chemical shifts and the areas of the peaks observed are shown in Table 1. The isotropic shift is very sensitive to the local surroundings of lithium ions, so the MAS NMR data allow us to determine non-uniformities at a level of chemical bond.

Due to the resolution of MAS spectra, the fine structure of the second component may be used to calculate the probability of population with $Ni^{3+}$ ions of the positions that are next to nearest ones with respect to the given lithium ion. The positions of the nearest neighbours of lithium contributing into this part of the spectrum are occupied only by $Co^{3+}$ ions. Let the amount of substituted neighbours in the second coordination sphere of the given lithium ion be $p_2$ ($0 \le p_2 \le 6$), and the probability of the occurrence of this amount of substituted neighbours ($1 - y$), where $q$ is the total probability of cobalt substitution with nickel, or the relative concentration of nickel in the sample, equal to ($1 - y$). For small $q$, most probably there are no substituted neighbours, so $P(q, 0) > P(q, 1)$. It may be demonstrated that for $q_0 = 1/7$ probability $P(q_0, 0) = P(q_0, 1)$. With further increase in nickel content, the probability of the absence of substituted neighbours becomes smaller than the probability to have even a single substituted cobalt atom. The $q$ values calculated from the experimental data using the least squares approximation, and the corresponding average error squared are listed in Table 1. One can see that nickel content does not exceed 0.1.

With an increase in nickel content $(1 - y) \ge 0.6$, the fine structure of MAS spectra disappears in the region corresponding to the absence of the nearest nickel ions (see Fig. 7). The data obtained are close to the results reported in [12] and provide evidence of the absence of uniform distribution of nickel ions in $Ni_{1-y}Co_yO_2$ layers for $0.6 \le (1 - y) \le 0.8$. Along with the observed discontinuity of the dependence of isotropic chemical shift on the composition of the sample (see Fig. 6) these data may be the evidence of the qualitative change of the character of ordering of Co and Ni ions in the $d$-metal layers for samples with $(1 - y) \ge 0.6$. Therefore, in the case of the high nickel content in the structure of $LiNi_{1-y}Co_yO_2$ microheterogeneity (microdomains) with nickel concentration up to 10 % is likely to appear, as well as the regions with its higher concentration that do not contribute into the highly resolved part of the spectrum. Such a deviation from the random distribution of Ni/Co has a narrow-local character and is not detected by means of XPA but may have a substantial effect on the electrochemical properties of cathode materials based on $LiNi_{1-y}Co_yO_2$.

The data obtained in electrochemical measurements of specific discharge capacity of $LiNi_{1-y}Co_yO_2$ samples depending on cycling rate (current density) are presented in Fig. 8. One can see that with an increase in nickel content in the sample the specific discharge capacity increases and reaches 170–180 mA · h/g for the composition $LiNi_{0.8}Co_{0.2}O_2$ at the cycling rate of $C/10$, which correlates with the litera-

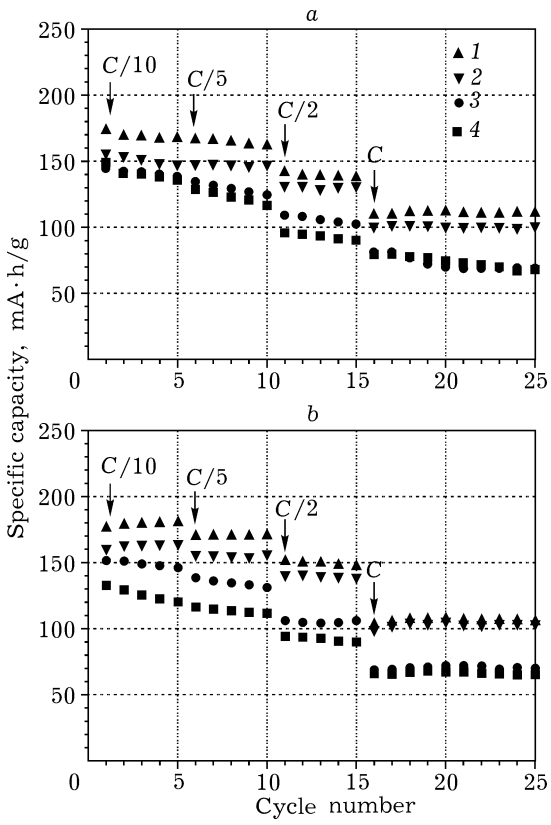


Fig. 8. Dependence of specific discharge capacity of $LiNi_{1-y}Co_yO_2$ samples obtained from hydroxides (*a*) and oxides (*b*) of nickel and cobalt on cycling rate ($C/10$, $C/5$, $C/2$ and $C$) and composition. The value of $y$: 0.2 (*1*), 0.4 (*2*), 0.6 (*3*), 0.8 (*4*).

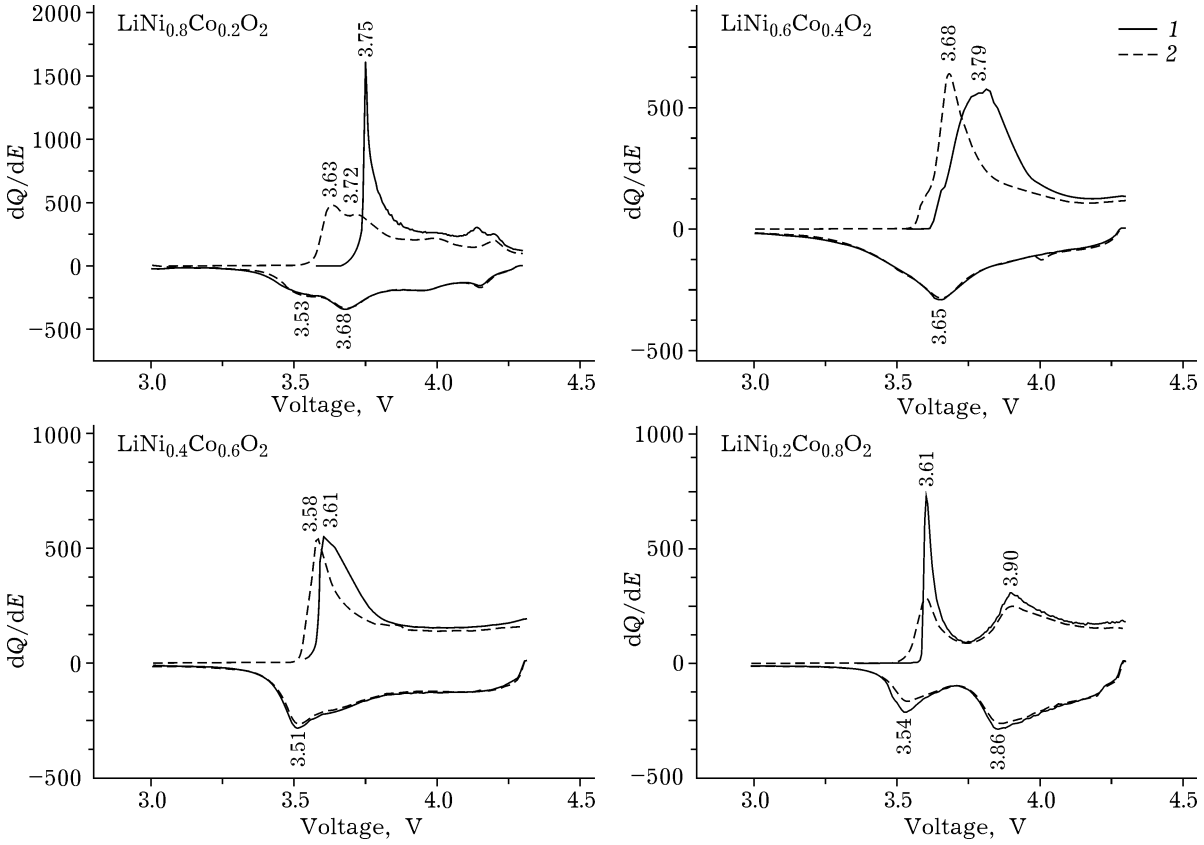


Fig. 9. Curves of differential capacity of $LiNi_{1-y}Co_yO_2$ obtained from nickel and cobalt hydroxides: *1, 2* – the first and the second cycles, respectively.

ture data for a similar composition (for example, [5]). At the minimal current densities (low cycling rates) the specific discharge capacity decreases smoothly with a decrease in nickel content of the samples; further on, the capacity of samples with $(1 - y)$ equal to 0.6 and 0.8 prepared both from nickel and cobalt hydroxides and oxides noticeably exceeds the capacity of the samples with $(1 - y) = 0.4$ and 0.2. Such a difference in the properties agrees with the data of NMR studies. It should also be noted that all the samples obtained are distinguished by the low ohmic resistance and polarization.

Analysis of the curves of differential capacity $dQ/dE = f(E)$ allowed us to follow the presence or absence of possible phase transitions during charge-discharge of the obtained $LiNi_{1-y}Co_yO_2$ samples. It may be assumed that the phase transitions characteristic of pure $LiNiO_2$ in the solid solutions $LiNi_{1-y}Co_yO_2$ are suppressed, but complete disappearance of structural rearrangements in the case of $LiNi_{0.8}Co_{0.2}O_2$ does not occur (Fig. 9). For the $LiNi_{0.2}Co_{0.8}O_2$ sample, sequential oxidation of $Ni^{3+}$ and $Co^{3+}$ ions is observed during charging: there are two redox peaks on the curves of differential capacity at 3.6 U ($Ni^{3+}/Ni^{4+}$) and 3.9 V ($Co^{3+}/Co^{4+}$) For the samples with higher nickel content, only one peak is observed. With a decrease in nickel content, the average voltage of oxidation-reduction peaks $Ni^{3+}/Ni^{4+}$ decreases from 3.75 (3.68) for $LiNi_{0.8}Co_{0.2}O_2$ ($LiNi_{0.6}Co_{0.4}O_2$) to 3.58 (3.51) for $LiNi_{0.4}Co_{0.6}O_2$ ($LiNi_{0.2}Co_{0.8}O_2$), which points to different electron states of $Ni^{3+}$ ions in the samples.

## CONCLUSION

Thus, it was demonstrated that cathode materials with good electrochemical properties were obtained with the help of mechanical activation at the stage of solid-phase synthesis of solid solutions $LiNi_{1-y}Co_yO_2$ ($y$ = 0.2, 0.4, 0.6, 0.8), with double hydroxides of nick-

el and cobalt used as the reagents, or the corresponding anhydrous oxides. Analysis of the fine structure of $^{6,7}$Li MAS NMR spectra allowed us to establish that nickel and cobalt ions in $Ni_{1-y}Co_yO_2$ layers for the samples with $60.6 \leq (1 - y) \leq 0.8$ are distributed nonuniformly. Such a deviation from the random distribution of Ni/Co has a narrow-local character and is not detected by means of XPA but affects the electrochemical properties of cathode materials.

## REFERENCES


1 A. Rougier, I. Saadoune, P. Gravereau *et al.*, *Solid State Ionics*, 90 (1996) 83.
2 C. Delmas, M. Menetrier, L. Croguennec *et al.*, *Electrochim. Acta*, 45 (1999) 243.
3 E. Zhecheva, R. Stoyanova, *Solid State Ionics*, 66 (1993) 143.
4 J. Molenda, P. Wilk, J. Marzec, *Ibid.*, 157 (2003) 115.
5 J. Cho, H. S. Jung, Y. C. Park *et al.*, *J. Electrochem. Soc.*, 147 (2000) 15.
6 K. K. Lee, K. B. Kim, *Ibid.*, 147 (2000) 1709.
7 G. X. Wang, J. Horvat, D. H. Bradhurst *et al.*, *J. Power Sources*, 85 (2000) 279.
8 N. Kosova, E. Devyatkina, *Solid State Ionics*, 72 (2004) 181.
9 M. Rajamathi, P. V. Kamath, R. Seshri, *J. Mat. Chem.*, 10 (2000) 503.
10 C. Faure, C. Delmas, M. Fouassier, P. Willmann, *J. Power Sources*, 35 (1991) 249.
11 C. Julien, in: Materials for Lithium-Ion Batteries, in C. Julien and Z. Stoyanov (Eds.), NATO Partnership Sub-Series 3: High Technology, vol. 85, Kluwer, Boston, 2000, p. 309.
12 C. Marichal, J. Hirshinger, P. Granger *et al.*, *Inorg. Chem.*, 34 (1995) 1773.
13 K. I. Gnanasekar, H. A. Cathrino, J. C. Jiang *et al.*, *Solid State Ionics*, 148 (2002) 299.
14 X. Guo, S. Greenbaum, F. Rouci, B. Scrosati, *Ibid.*, 168 (2004) 37.